Annals of R.S.C.B., ISSN:1583-6258, Vol. 25, Issue 4, 2021, Pages. 910 - 928
Received 05 March 2021; Accepted 01 April 2021.

Synthesis, Characterization and DFT Studies of New Azo-Schiff Base and Evaluation as Corrosion Inhibitor

Samia Mezhr Merdas*
*Department of Chemistry, College of Science, University of Thi-Qar, Iraq.
*Corresponding Author E-mail: samia.m_mschem@sci.utq.ed..u.iq , samiy4692@gmail.com

ABSTRACT:

A new Azo-Schiff base namly 6,6'-((1E,1'E)-(1,2- phenylenebis (azanylylidene)) bis (methanylylidene)) bis(3-(o-tolyldiazenyl)phenol) (A_1) have been synthesized and characterized by elemental analysis, FT-IR,^{1}H-NMR and Mass spectra. The new compound was evaluated as corrosion inhibitor for brass alloy in 0.5 M HCl, using weight loss . Weight loss measurements was studied at different temperatures and concentration and results show that the inhibition efficiency increases with decreasing temperature and increasing concentration of inhibitors and the highest inhibition efficiency was obtained at an optimum concentration of (1×10^{-3} M) for inhibitor at 298 K . Thermodynamic parameters enthalpy of activation (ΔH_a^*) , entropy of activation (ΔS^*_a), and the activation energy (Ea) and for brass alloy corrosion and inhibitor adsorption, respectively, were determined and discussed. It has been determined that the adsorption for the studied inhibitors on brass complies with the Langmuir adsorption isotherm at 298 K, the calculated ΔG_{ads} values were found to be around -35 kJ mol^{-1}, which indicates that inhibitor (Azo-Schiff base) is adsorbed on the brass surface by chemical and physical interactions. For further investigations DFT studies were employed to study the electrostatic potential and explain the nature of interaction between the inhibitor molecules and metal surface.

Keywords: Azo-azomethine, synthesis, corrosion inhibitors, Adsorption, Thermodynamic parameters

INTRODUCTION:

Corrosion problems have received a considerable amount of attention because of their economic and safety consequences .The use of inhibitors is one of most practical methods for protection against corrosion[1]. Corrosion commonly occurs at metal surfaces in the presence of oxygen and moisture , involving two electrochemical reactions ,oxidation takes place at anodic site and reduction occurs at cathodic site , In acidic medium hydrogen evolution reaction predominates and corrosion inhibitors reduce or prevent these reactions[2]. Generally the organic compounds containing hetero atoms like O,N,S and P are found to work as very effective corrosion inhibitors [3-5].The efficiency of these compounds depends upon electron density present around the hetero atoms [6] . The number of adsorption active centers in the molecule and their charge density ,molecular size ,mode of adsorption and formation of metallic complexes[2].

Azo derivatives are organic compounds that contain –N=N– bridge in their structure, most of these compounds are used as synthetic dyes, furthermore, many of them have been reported as compounds with interesting applications in different fields such as pharmaceuticals, cosmetics and corrosion inhibitors [7-9]. The presence of the nitrogen

Annals of R.S.C.B., ISSN:1583-6258, Vol. 25, Issue 4, 2021, Pages. 910 - 928
Received 05 March 2021; Accepted 01 April 2021.

atoms in the azo linkage and the flexibility in choosing the other moieties in the structures of the azo dyes make it possible to design molecules that have the structural requirements of the organic corrosion inhibitors which are readily and strongly adsorbed on the metals surface. 10. The aim of the present study is to Synthesis of new azo-Schiff bases, Studying efficiency of the Schiff bases in inhibiting brass corrosion in acidic media (0.5 N HCl) and Studying efficiency of new azo-Schiff base in inhibiting brass corrosion by weight loss methods .

MATERIAL AND METHODS:

Chemicals and reagents:

All analytical grade reagents were used without further purification as received from different company. Acetic acid (glacial) (99.5%), O-toluidine (99.0%), NaOH (99.0%), HCl (37%), $NaNO_2$, (99%) were purchased from BDH and O-phenylenediamine (99.5%) and Salicylaldehyde (99.0%) from sigma Aldrich.

Instrumentation:

The UV-Vis spectrophotometer model T 60, PG Instruments Ltd, (Germany). The FT-infrared measurements were recorded by using FT-IR affinity Spectrophotometer (Shimadzu) Japan; Mass spectra are recorded of compounds using Agilent Technology (HP)/MS Model 5973 Network Mass Selective Detector and element analysis model Eager 300 for EA1112 in the University of Tehran, Iran. The ^{1}H-NMR with using DMSO as solvent in Tehran, Iran.

Preparation of new Azo-schiff base(A1):

Azo dye **(2-hydroxy-4-(o-tolyldiazenyl)benzaldehyde**) was prepared by dissolving (2.143gm, 0.02 mole) of O-toluidine in mixture containing 30ml distilled water and 5ml of concentrated hydrochloric acid and cooled to (0-5)^{o}C. The solution was diazotized at (0-5) ^{o}C with (1.38gm, 0.02 mole) sodium nitrate was dissolved in 20 ml distilled water was added drop wise to amine solution and stirring continuously at (0-5)^{o}C and left to stand 30 min. This diazonium solution was added to salicylaldehyde (2.442gm, 2.13ml, 0.02mol) was dissolved in 25ml ethanol and 30 ml of 6% sodium hydroxide. The mixture was stirred continuously for 2h. at (0-5)^{o}C in ice-bath and allowed to stand in the refrigerator overnight and acidified with dilute hydrochloric acid to pH=6. The precipitate was filtered and washed with distilled water and ethanol solution to remove the excess of unreacted substances and recrystallized from ethanol and dried in oven at 50^{o}C for two hours[11,12].The purity was confirmed by TLC technique. Yield 90.44%, mp 112-113˚C. The Schiff base was prepared from condensation eaction by dissolving (2.403gm,0.01mol) of **(**2-hydroxy-4-(o-tolyldiazenyl)benzaldehyde) in (20 ml) absolute methanol then mixed with a solution(0.541gm, 0.005mol) of (O-phenylenediamine) dissolved in (10ml) of the same solvent with the addition of four drops of glacial acetic acid as a catalyst followed by reflux for 5 hours. The reaction was followed using TLC [13,14], Yield 84.56%, mp 243-245˚C. The dark brown precipitate was formed it was filtered, dried and recrystallized in absolute ethanol. The reaction is shown in Fig. 1.

Annals of R.S.C.B., ISSN:1583-6258, Vol. 25, Issue 4, 2021, Pages. 910 - 928
Received 05 March 2021; Accepted 01 April 2021.

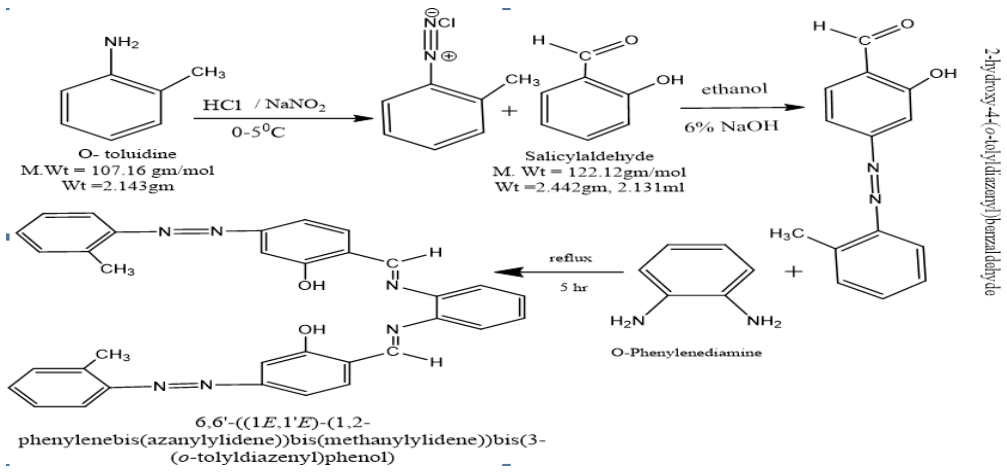

Figure.1 Preparation of new Azo-schiff base(A1)

Weight loss measurements

Corrosion tests were performed using coupons prepared from brass alloy. The chemical composition (wt %) of the brass alloy sample in Table.1

Table 1. The chemical composition (wt %) of the brass alloy sample

Metals	Cu	Zn	Al	Fe	As	Other
wt %	68.75	28.00	1.20	1.00	0.05	1.00

The aggressive acid solutions were made from analytical grade hydrochloric acid (HCl). Appropriate concentration of acid (0.5 M HCl) were prepared by using deionised water and used in absence and presence of certain inhibitor concentrations (1×10^{-3}M to 1×10^{-6} M) at immersion time(1-5) h and different temperatures(298,308,318) K . The corrosion rate (CR) , the percentage inhibition efficiency (IE %) and the degree of surface coverage (θ) were calculated using the following equations [15,16]:

.....(1)

$$\mathbf{CR=}\frac{WL.K}{A.t.D}$$

Where:

WL is the weight loss (g) before and after immersion in the test solutions CR is the corrosion rate

A is the area of the specimen (Inch^2) D is the density of the alloy in gcm^{-3}

K is a constan (543) (giving rate in mpy) and t is immersion time (hours).

The inhibition efficiency(IE%)was computed using the following equation[15,16]:

$$\mathbf{IE\%=}\frac{CR_{uninh}-CR_{inh}}{CR_{unih}}\mathbf{\times 100} \quad \text{.....(2)}$$

Annals of R.S.C.B., ISSN:1583-6258, Vol. 25, Issue 4, 2021, Pages. 910 - 928
Received 05 March 2021; Accepted 01 April 2021.

Where:

CR uninh and CR inh are the corrosion rates in the absence and presence of the inhibitor ,respectively θ is the surface coverage of the metal surface covered by the adsorbed inhibitor, was evaluated from weight loss measurements using the following equation[15,16]: **…….(3)**

$$\theta = \frac{CR_{uninh} - CR_{inh}}{CR_{uninh}}$$

Quantum chemical calculations:

The quantum chemical calculations were carried out with complete geometry optimization by using density functional theory (DFT) method at B3LYP/6 -31++ G(d, p) level by using Gaussian 09W which connected with Gauss View 5.0 in order to calculate the most important parameters such as E_{HOMO}, E_{LUMO}, energy gap (ΔE) and the other parameters that influence the nature of interaction between the inhibitor molecule and the alloy surface.

Results and Discussion

Element analysis

The elemental analysis was tabulated in **Table 2** , The calculated values were in a good agreement with the experimental values.

Table 2. Elemental analysis data of the prepared Azo-schiff base(A1)

Ligand	Molecular Weight	Experimental			Theoretical		
		C%	H%	N%	C%	H%	N%
A_1	552	73.901	5.050	15.193	73.913	5.072	15.217

FT-IR spectrum

The IR spectrum was obtained for analytical reagent prepared as KBr in **Fig.2**. The spectra show absorption band in 3294 cm^{-1} belong to OH [17]. The absorption band at 1612cm^{-1}belong to stretching vibration of C=N of imine[18] and a strong band in the range at 1543 Cm^{-1} due to the stretching vibration of the (N=N) [19]. The C=C appear stretching vibration at 1489 cm^{-1} [20]. But stretching vibration for the C-H aromatic appear weak band at 3062 cm^{-1} [19], absorption band at 2970 cm^{-1} due to C-H aliphatic [18].

Annals of R.S.C.B., ISSN:1583-6258, Vol. 25, Issue 4, 2021, Pages. 910 - 928
Received 05 March 2021; Accepted 01 April 2021.

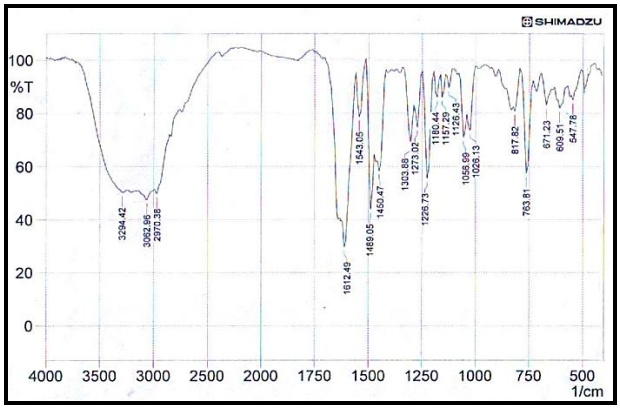

Figure2. IR spectrum for the prepared Azo-schiff base(A1)

^{1}H-NMR spectrum

The ^{1}H-NMR spectrum of the prepared Azo-schiff base(A1)was recorded in DMSO (δ at 2.56) as solvent in**Fig 3**. The chemical shift δ ppm at 6.78-7.33 (m,18H, aromatic rings) [17], δ at 3.76 (s,6H, CH_3) [21], δ at 7.64 (m,2H,2OH) and 7.75 (m, 2H, 2CH=N) [17].

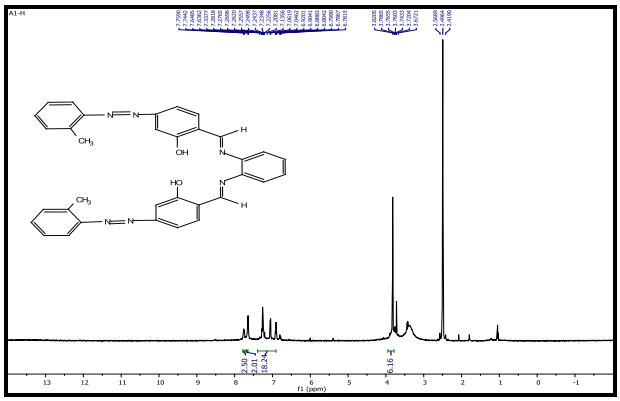

Figure 3. ^{1}H-NMR spectrum for the prepared Azo-schiff base(A1)

Mass spectrum

The mass spectrum of the prepared Azo-schiff base(A1) was recorded and the obtained molecular ion (m/z) peaks confirm its proposed formula and geometry. The ligand shows a peak at M^{+}=552 corresponding to the molecular ion peak ($C_{34}H_{28}N_6O_2$) in the figure (5). It also showed a series of peaks at m/z = 433, 313, 237, 223, ,210, 195, 119, 105, 91, 77 and 65 corresponding to $[C_{27}H_{21}N_4O_2]^{+}$,$[C_{20}H_{13}N_2O_2]^{+}$,$[C_{14}H_{11}N_3O]^{+}$, $[C_{14}H_{11}N_2O]^{+}$,$[C_{13}H_{10}N_2O]^{+}$, $[C_{13}H_9NO]^{+}$, $[C_7H_7N_2]^{+}$, $[C_7H_7N]^{+}$,$[C_7H_7]^{+}$, $[C_6H_5]^{+}$ and $[C_5H_5]^{+}$, respectively **(Fig 4**).

Annals of R.S.C.B., ISSN:1583-6258, Vol. 25, Issue 4, 2021, Pages. 910 - 928
Received 05 March 2021; Accepted 01 April 2021.

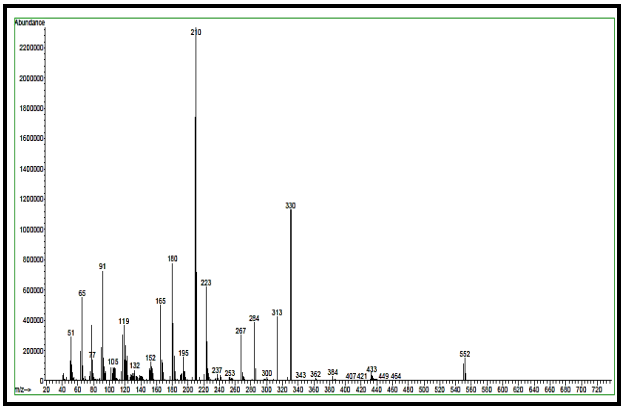

Figure 4. Mass spectrum for Ligand (A_1)

Weight loss measurements

Effect of inhibitor concentration on corrosion process

Weight loss data and the rate of corrosion of brass alloy in 0.5 M HCl in the absence and presence of various concentrations of inhibitors at 298 K after 4 h immersed period were obtained and are given in **Table 3.** The results show that the weight loss data and the rate of corrosion decrease with increasing inhibitor concentration [22-25] **(Figs. 5 and 6)**. .

Table 3.Weight loss and Corrosion rate for brass alloy in 0.5M HCl in the absence and presence of various concentrations of inhibitor at 298 K after 4 h immersed period

Inhibitor conc.(M)	weight loss (g)	Corrosion rate (mpy)
0	0.0084	47.5
1×10^{-6}	0.0050	28.2
1×10^{-5}	0.0036	20.3
1×10^{-4}	0.0032	18.1
1×10^{-3}	0.0024	13.5

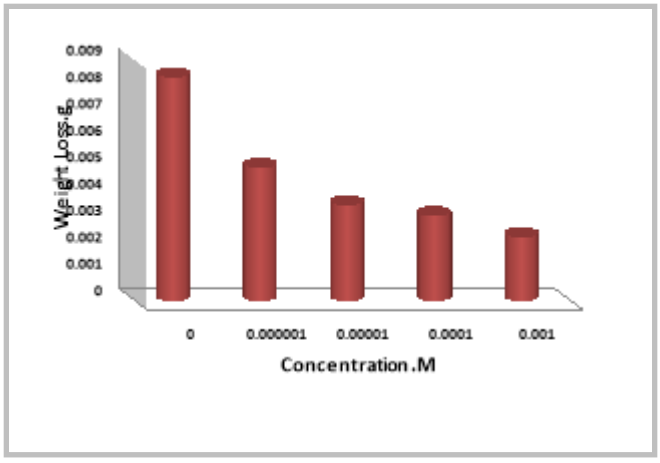

Figure 5. Weight loss Vs. Concentration at 298K after 4 h immersed period

Annals of R.S.C.B., ISSN:1583-6258, Vol. 25, Issue 4, 2021, Pages. 910 - 928
Received 05 March 2021; Accepted 01 April 2021.

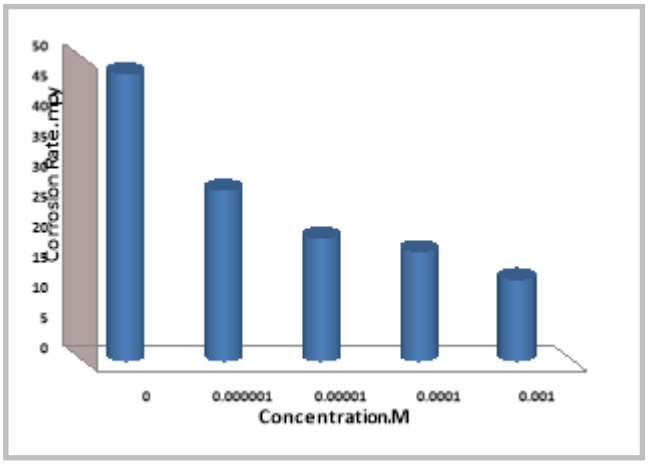

Figure 6. Corrosion rate Vs. Concentration at 298K after 4 h immersed period

Effect of immersion Time on corrosion process

The effect of addition of inhibitor on the corrosion of brass alloy in 0.5 M HCl solution was studied by weight loss method at 298 K after (1-5) h of immersed period in the absence and present of (1×10^{-3} M) of the prepared azo-Schiff base as inhibitor corrosion and are shown in **Figs. (7 and 8) .**The figures clearly show a great reduction in weight loss and the rate of corrosion with the increase in immersion from 1h to 5 hat different temperature of the metal coupons in the presence of the inhibitor compared to the hydrochloric solutions alone. This is due to the formation of strong passive protective layer on the surface of the metal when exposed to electrolyte for more time [26-28] . The values of Weight loss (g) and corrosion rate (mpy) are summarized in **Table 4.**

.

Table 4.Weight loss and corrosion rate for brass alloy in 0.5 M HCl in the absence and presence of inhibitor(A1) (c= 1×10^{-3}M) in the different immersion at time 298K

The Variable	Corrosion Medium	Immersion Time(hours)				
		1	2	3	4	5
Weight loss (g)	HCl only	0.0040	0.0065	0.0073	0.0084	0.0086
Corrosion rate (mpy)	HCl only	90.50	73.53	55.05	47.51	38.91
Weight loss (g)	HCl+ inhibitor	0.0002	0.0014	0.0020	0.0024	0.0031
Corrosion rate (mpy)	HCl+ inhibitor	4.52	15.83	15.08	13.5	13.02

Annals of R.S.C.B., ISSN:1583-6258, Vol. 25, Issue 4, 2021, Pages. 910 - 928
Received 05 March 2021; Accepted 01 April 2021.

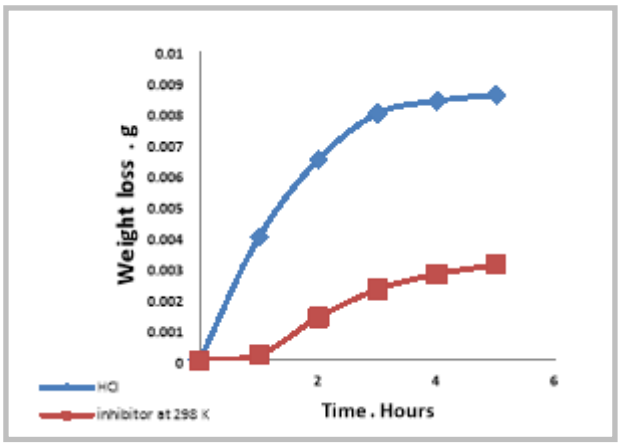

Figure 7. Weight loss Vs. Immersion Time at 298K

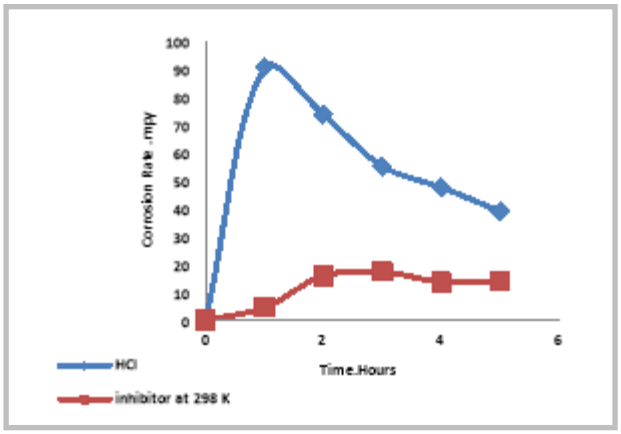

Figure 8.Corrosion rate Vs. Immersion Time at 298K

Effect of temperature

To evaluate the adsorption of inhibitor and activation parameters of the corrosion process of brass alloy in acidic medium, weight loss measurements were done at (298,308,318) K, in the absence and presence of inhibitor at concentration (1×10^{-3}M) during 4 hr. immersion time. The variation of inhibition efficiency and Surface coverage with inhibitor with temperature is given in **Figs (9 and 10**) .The effect of temperature on the inhibited acid-metal reaction is very complex. Many changes such as rapid etching desorption of inhibitor, as well as inhibitor decomposition occur on the metal surface [29]. The results revealed that, on increasing temperature, there is a decrease in inhibition efficiency for compound used. Generally, the metallic corrosion in acidic media is accompanied with evolution of hydrogen gas, and rise in the temperature usually accelerates the corrosion reactions resulting in higher dissolution rate of the metal [30]. A decrease in inhibitor efficiency with temperature can be attributed to the increased desorption of inhibitor molecules from the metal surface, or decreased adsorption process strength at elevated temperature suggesting a physical adsorption mode. Temperature investigations are also required, although they do not furnish all of the information needed for the elucidation of adsorption character. There are cases in which

Annals of R.S.C.B., ISSN:1583-6258, Vol. 25, Issue 4, 2021, Pages. 910 - 928
Received 05 March 2021; Accepted 01 April 2021.

chemical adsorption is accepted, although inhibition efficiency decrease with increasing temperature [31]. .

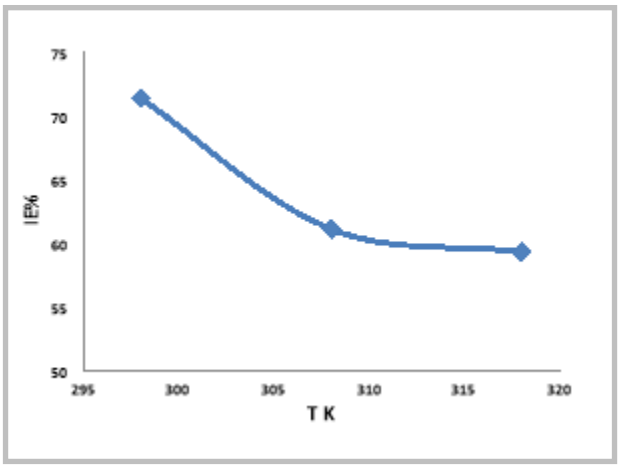

Figure 9. Inhibition efficiency of inhibitor (c= 1×10^{-3}M) in 0.5M HCl at different temperatures

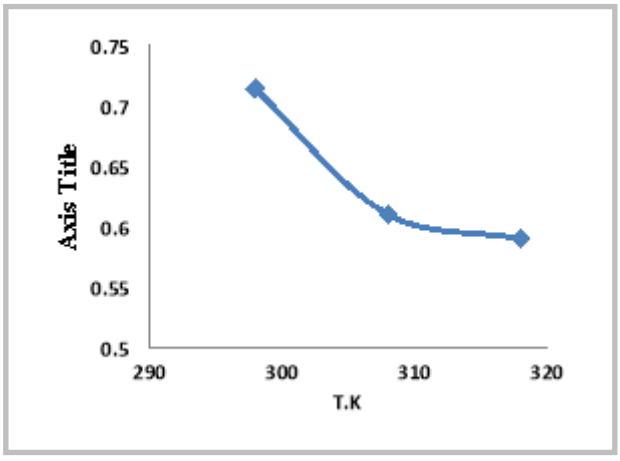

Figure 10. Surface coverage with inhibitor (c= 1×10^{-3}M) in 0.5M HCl at different temperatures

Thermodynamics parameters and Activation energy

Activation energy (Ea)

The values of activation energy (Ea) for brass alloy corrosion reaction were obtained from Arrhenius equation(4):

$$\log\frac{CR_2}{CR_1} = \frac{E_a}{2.303R}\left(\frac{1}{T_1}-\frac{1}{T_2}\right) \qquad \text{.....(4)}$$

where CR_1 and CR_2 are corrosion rates at temperatures T_1 and T_2, respectively and Ea is the apparent activation energy for corrosion process which represents the energy necessary for a molecule to possess in order to react [32]. The values of Ea are given in **Table 5**. It is found that Ea values for inhibited systems are higher than Ea for uninhibited systems. The increase in activation energy after the addition of the inhibitor

Annals of R.S.C.B., ISSN:1583-6258, Vol. 25, Issue 4, 2021, Pages. 910 - 928
Received 05 March 2021; Accepted 01 April 2021.

to acid solutions can indicate that physical adsorption (electrostatic) occurs in the first stage. Physical adsorption is small but important because it is preceding stage of chemisorption of investigated organic compounds on brass alloy surface [33]. The increase in the activation energy also indicates a strong adsorption of the inhibitor molecules on brass alloy surface .

Enthalpy and Entropy of activation

The values of enthalpy and entropy of activation can be calculated from the alternative form of Arrhenius equation(5) as follows:

$$log\frac{CR}{T} = [log(\frac{R}{Nh}) + (\frac{\Delta S_a^*}{2.303R})] - (\frac{\Delta H_a^*}{2.303RT}) \quad \text{.....(5)}$$

where h is Planks constant, N is Avogadro's number, ΔS_{a^*} is the entropy of activation, and ΔH_{a^*} is the enthalpy of activation. . A plot of log CR /T versus 1/T should give straight lines (**Fig.11**),with a slope of ($-\Delta H_{a^*}$ /2.303R), and an intercept of [log(R/Nh)+(ΔS_{a^*} /2.303R)],from which the values of ΔH_{a^*} and ΔS_{a^*} were calculated, respectively .The value of ΔH_{a^*} is reported in **Table 5** and is positive. The positive sign of the enthalpy reflects the endothermic nature. Also, the value of entropy of activation is negative. The negative value of entropy implies that the activated complex in the rate determining step represents an association rather than dissociation step, meaning that a decrease in disordering takes place on going from reactant to activated complex [34,35] .

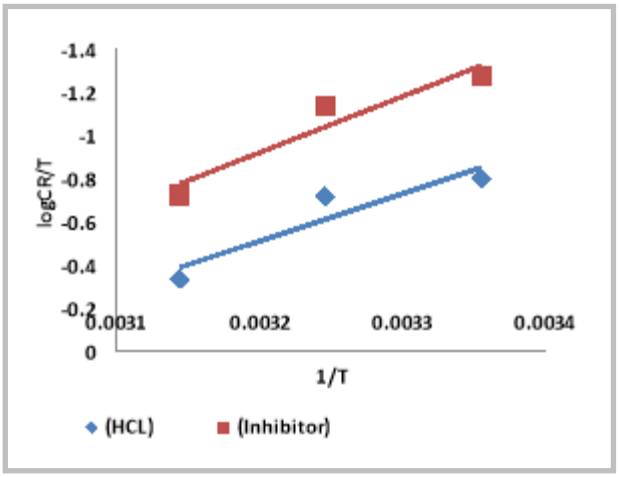

Figure 11. Alternative Arrhenius plots of brass dissolution in 0.5M HCl in the absence and presence of 10^{-3} M of inhibitor

Annals of R.S.C.B., ISSN:1583-6258, Vol. 25, Issue 4, 2021, Pages. 910 - 928
Received 05 March 2021; Accepted 01 April 2021.

Table 5. Thermodynamics parameters and Activation energy for brass alloy dissolution in acid solution in absence and presence of Inhibitor[the prepared Azo-schiff base(A1)]

Corrosion medium	$\Delta Ha*$(kJmol$^{-1)}$	$\Delta Sa*$(Jmol^{-1} K^{-1})	Ea(kJmol^{-1})
only HCl	42.1	-72.6	-74.8
HCl + Inhibitor	49.8	-55.8	-80.6

Adsorption Studies

The study of adsorption isotherms gives an idea about the adsorptive behavior of the inhibitor molecule which can provide important information about the nature of the metal-inhibitor interaction. Two main types of interaction can describe the adsorption of the organic compounds are physical adsorption and chemical adsorption. These are influenced by the chemical structure of the inhibitor, the type of the electrolyte, and the charge and nature of the metal. Several adsorption isotherms were tested to fit with the experimental data. These include the Langmuir, Frumkin, Temkin, Freundlich , and Flory-Huggins isotherms. The best fit was obtained from the Langmuir isotherm. The Langmuir isotherm equation(6) is of the following form:

.

$$\frac{\theta}{1-\theta} = K_{ads} .C \quad \text{.....(6)}$$

where c is the inhibitor concentration in mol dm^{-3}, θ the surface coverage and K_{ads} is the equilibrium constant of adsorption process. The equilibrium constant for the adsorption process(K_{ads}) is related to the standard Gibbs free energy of adsorption(ΔG_{ads})by the following equation(7): :

.....(7)

$$\Delta G_{ads} = -RT \ln (55.5\ K_{ads})$$

where 55.5 mol dm^{-3} is the molar concentration of water in the solution, R is the gas constant and T is the absolute temperature [36]. The negative ΔGads values (**Table 6**) are consistent with the spontaneity of the adsorption process and the stability of the adsorbed layer on the mild steel surface [37] . It has been reported[38] that the values of ΔG_{ads} up to −20kJmol^{-1} the adsorption was regarded as physisorption ,the inhibition acts due to the electrostatic interaction between the charged molecules and the charged metal and more than -40 kJ mol^{-1} indicate chemisorption (charge sharing and/or electron transfer between the orbitals of the inhibitor molecules and those of the metal to form co–ordinate bonding) [39]. It is suggested that the adsorption of inhibitor investigated involves chemisorption process. However, some researchers have reported [40] that adsorption of inhibitor molecules is not merely physisorption or chemisorption but obeying a comprehensive adsorption (physical and chemical adsorption) for the same value. However, which kind of adsorption will play a more important role in the corrosion inhibition would be discussed further.

Annals of R.S.C.B., ISSN:1583-6258, Vol. 25, Issue 4, 2021, Pages. 910 - 928
Received 05 March 2021; Accepted 01 April 2021.

Table 6. Parameters for adsorption of inhibitor in barss/inhibitor/0..5M HCl system at 298 K

Temperature(K)	K_{ads} $(10^4)M^{-1}$	ΔG_{ads} kJ mol^{-1}	R^2
298	1645.5	-28.3	0.901

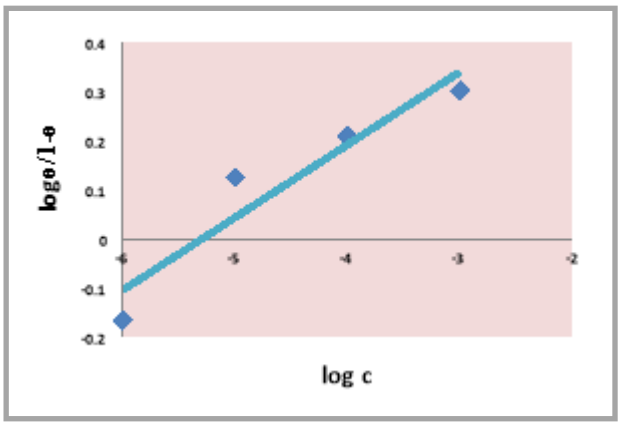

Figure 12. Langmuir's adsorption plots for brass alloy in 0.5 M HCl with various concentrations of compounds studied at 298K

4. Quantum chemical calculations

Quantum chemical methods are useful in determining the molecular structure as well as elucidating the electronic structure and reactivity [41]. Therefore, it has become a common practice to carry out quantum chemical calculations in the field of corrosion inhibition studies. These lection of effective and appropriate inhibitors for the corrosion of metals has been widely carried out based on empirical approach [42, 43]. Computational methods are used to understand and explain the functions of organic compounds in molecular terms. In the present study, quantum chemical calculations were performed for investigating the relationship between the molecular structures of and inhibition effect on the brass surface by DFT studies. The highest occupied molecular orbitals (HOMO) populations and lowest unoccupied molecular orbitals (LUMO) for the prepared Azo-schiff base is shown in **Figs. 14 and 15**. The tendency of the molecule to donate and accept electrons is related to the energy levels of HOMO and LUMO respectively, the higher HOMO energy level (E_{HOMO}) is higher in donation ability and the lower LUMO energy level (E_{LUMO}) is higher in acceptance ability, so, the lower energy band gap ($\Delta E = E_{LUMO} - E_{HOMO}$) leads to stronger interactions between the molecule and the metal surface through the donation and acceptance of electrons, in other words, higher inhibition efficiencies due to the formation of the protective film through the adsorption of the inhibitor molecules onto the metal surface [44, 45], that an increase in the values of E_{HOMO} and a decrease in E_{LUMO}- E_{HOMO} values cause increase in the inhibitive action of the studied Schiff bases. It is known that in the chemical adsorption an increase in E_{HOMO} values causes a significant increase in the inhibition

Annals of R.S.C.B., ISSN:1583-6258, Vol. 25, Issue 4, 2021, Pages. 910 - 928
Received 05 March 2021; Accepted 01 April 2021.

efficiency of organic compounds [46,47]. On the other hand, the energy gap between E_{LUMO} and E_{HOMO} can be used as a characteristic quantity for metallic complexes [48-50]. The lower energy gap indicates the higher stability of the formed complex, thus the higher inhibition efficiency. E_{HOMO} and E_{LUMO} of the inhibitor molecule are related to the ionization potential (I) and the electron affinity (A), respectively. The ionization potential and the electron affinity are defined as $I = - E_{HOMO}$ and $A = - E_{LUMO}$, respectively. Then absolute electronegativity (χ) and global hardness (η) of the inhibitor molecule are approximated as follows [51] :

$$\chi = (I+A)/2 \quad \text{.....(8)}$$

$$\eta = (1-A)/2 \quad \text{.....(9)}$$

The softness (s) was computed through following equation [10]:

$$\sigma = 1/\eta \quad \text{.....(10)}$$

The global electrophilicity index was introduced by Parr [52] and is given by:

$$\omega = \mu^2/2\eta \quad \text{.....(11)}$$

Thus the fraction of electrons transferred from the inhibitor to metallic surface, ΔN, is given by [53]:

$$\Delta N = \square_{cu} - \square_{inh} / 2(\eta_{Cu} + \eta_{inh}) \quad \text{.....(12)}$$

In order to calculate the fraction of electrons transferred, a theoretical value for the electronegativity of bulk copper was used χ_{Cu}= 4.48 eV/mol [54], and a global hardness of , η_{Cu} = 0 eV/mol by assuming that for a metallic bulk I = A [55] because they are softer than the neutral metallic atoms. A positive ΔN value means the ability of an inhibitor molecule to share its electrons and vice-versa for a negative value. According to hard and sofe acid base concept [56] , a smaller value of global hardness(η) and the dipole moment (μ) , showed higher inhibition efficiency quantum chemical parameters obtained from the calculations which are responsible for the inhibition efficiency of inhibitors [51] , such as the highest occupied molecular orbital (E_{HOMO}), energy of lowest unoccupied molecular orbital (E_{LUMO}), HOMO–LUMO energy gap (ΔE_{H-L}), dipole moment (μ) and total energy (TE), electronegativity (χ), electron affinity (A), global hardness (η), softness (σ), ionization potential (I), The global electrophilicity (ω), the fraction of electrons transferred from the inhibitor to iron surface (ΔN) and the total energy (TE) for the prepared Azo-schiff base, are collected in **Table 7 .**

Table7. Selected quantum chemical parameters for the prepared Azo-schiff base(A1)

Parameters (ev)	Inhibitor
E_{LUMO}	**-2.25**
E_{HOMO}	**-4.61**
Energy band gap($\Delta E = E_{LUMO} - E_{HOMO}$)	**2.36**
Dipole moment μ (Debye)	**5.22**
Ionization potential($I = - E_{HOMO}$)	**4.61**

Annals of R.S.C.B., ISSN:1583-6258, Vol. 25, Issue 4, 2021, Pages. 910 - 928
Received 05 March 2021; Accepted 01 April 2021.

Electron affinity(A = -E_{LUMO})	**2.25**
Chemical hardness (η= (I-A)/2)	**1.18**
Chemical softness σ=(1/ η)	**0.85**
Electronegativity (χ = (I+A)/2)	**3.44**
Chemical potential (μ = -(I+A)/2)	**-3.44**
Electrophilicity index(ω =μ^2/2 η)	**5.001**
ΔN= □$_{cu}$-□$_{inh}$/ 2(η_{Cu}+ η_{inh})	**0.619**
The total energy (TE)	**-48725.25**

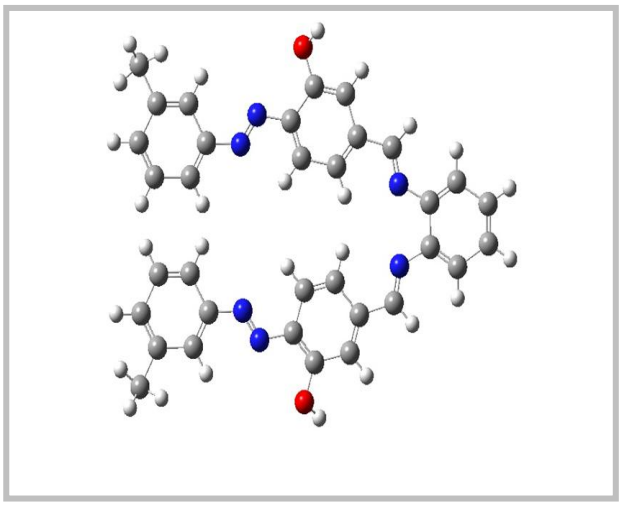

Figure 13.Optimized structure of the prepared Azo-schiff base(A1)

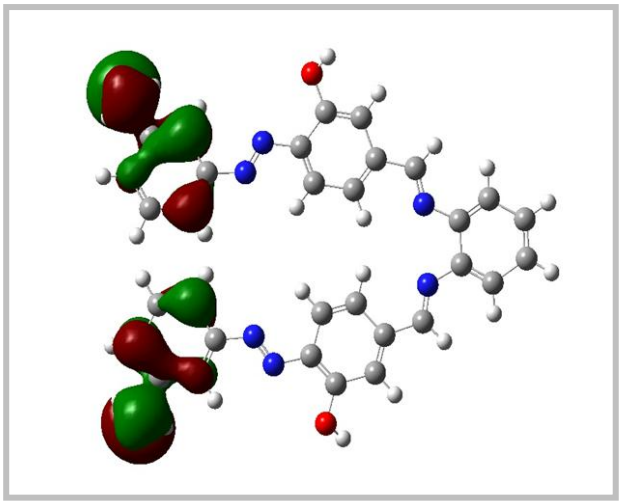

Figure 14. The highest occupied molecular orbitals (HOMO) electron density surfaces for the prepared Azo-schiff base(A1)

Annals of R.S.C.B., ISSN:1583-6258, Vol. 25, Issue 4, 2021, Pages. 910 - 928
Received 05 March 2021; Accepted 01 April 2021.

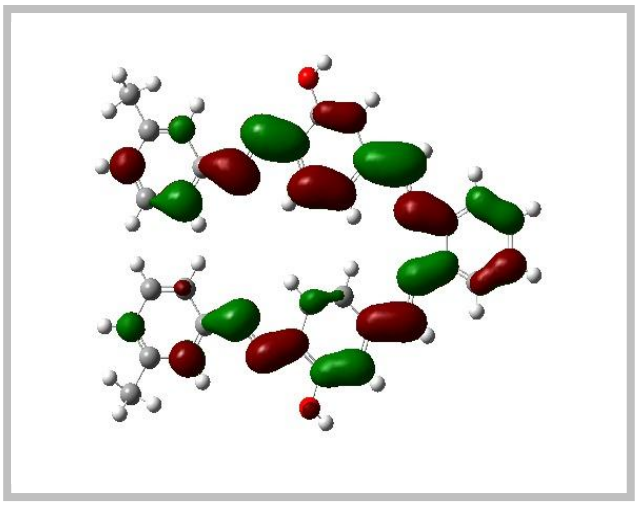

Figure 15.The lowest unoccupied molecular orbitals (LUMO) electron density surfaces for the prepared Azo-schiff base(A1)

Molecular Electrostatic Potential (MEP)

Molecular Electrostatic potential is very important in finding the active site in the molecule system with a positive point charge. The species that have positive charge tend to attack a molecule where the electrostatic potential is strongly negative (electrophilic attack). Electrostatic potential of inhibitor was measured and plotted as 2D contour to find the active site of molecule [57] as shown in **Fig.16 .**

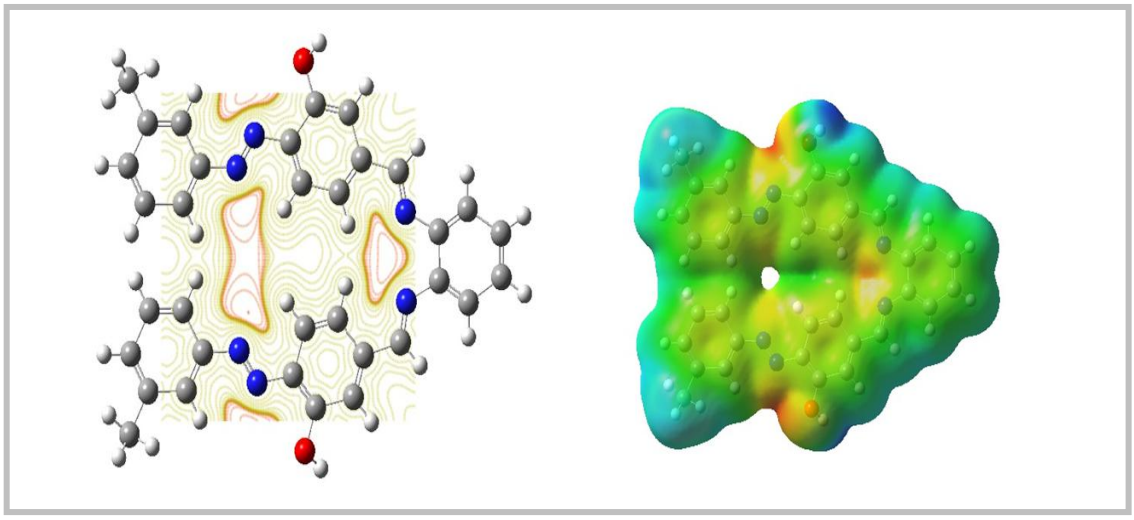

Figure 16.Electrostatic Potential for the prepared Azo-schiff base(A1)

Annals of R.S.C.B., ISSN:1583-6258, Vol. 25, Issue 4, 2021, Pages. 910 - 928
Received 05 March 2021; Accepted 01 April 2021.

Conclusion

A new Azo-Schiff base namly 6,6'-((1E,1'E)-(1,2- phenylenebis (azanylylidene)) bis (methanylylidene)) bis(3-(o-tolyldiazenyl)phenol)(A1)presents good effectiveness in 0.5 N HCl and even at higher temperature . The inhibition efficiency increments with rise of time and diminishes with temperature .The adsorption of the prepared compound follows the Langmuir's adsorption. The adsorption of inhibitor molecules on the brass alloy is not merely physisorption or chemisorption but obeying a comprehensive adsorption (physical and chemical adsorption) for the same value, while the negative value of show the spontaneity of the adsorption process.

References

[1] K.f.khaled , J .Int. Electrochem .sci ,3,462,2008.

[2] T. Sethi, A. Chaturvedi , J. Chil. Chem. Soc., 52, 3 , 2007.

[3]W. Quafsaoui, C.H. Blanc, N. Bebere, J.APPl.Electrchem ,30,959,2000.

[4]C. Blanc, S. Gastaud, J. Electrochem. Soc. 150, 396 ,2003.

[5] E. E. Ebenso, P. C. Okafor, U. J. Eppe, Anti Corr. Meth. and Mat, 50,414 ,2003.

[6]G. Bereket, A. Yurt, S. ustun Kandemir, 5th Advanced Batteries and Accumulators ABA (2004).

[7] D. Clofent, M. De Homdedeu, M. Munõz-Esquerre, M.J. Cruz, X. Munõz, Sudan red dye: A new agent causing type-2 occupational asthma, Allergy, Asthma Clin. Immunol. 16 (2020) 1–3.

[8]F. Vázquez-Ortega, I. Lagunes, Á. Trigos, Cosmetic dyes as potential photosensitizers of singlet oxygen generation, Dye. Pigment. 176 (2020).

[9]L.H. Madkour, S. Kaya, L. Guo, C. Kaya, Quantum chemical calculations, molecular dynamic (MD) simulations and experimental studies of using some azo dyes as corrosion inhibitors for iron. Part 2: Bis–azo dye derivatives, J. Mol. Struct. 1163 (2018) 397–417.

[10]A.S. Fouda, M.M. Mukhtar, New arylazodyes as corrosion inhibitors for mild steel in HCL solution, Chem. Eng. Commun. 198 (2011) 1111–1128

[11] Erdem, E., Sari, E. Y., Kilinçarslan, R., & Kabay, N. (2009). Synthesis and characterization of azo-linked Schiff bases and their nickel (II), copper (II), and zinc (II) complexes. Transition metal chemistry, 34(2), 167-174.

[12] Affat, S. S., & Al-Shamkhawy, S. (2018). Synthesis, Characterization and Spectroscopic Studies of a6, 6'- ((1E, 1'E)-(1, 2-phenylene bis (azanylylidene)) bis (methanylylidene)) bis (3-(phenyldiazenyl) phenol) and their Complexes. Journal of Global Pharma Technology, 10(10), 207- 221.

[13]Mehdi, R. T., & Hussen, S. A. (2011). Preparation, Idendetification and study of The biological activity of Co (II), Ni (II) and Cu (II) with the New Ligand1-[(4-

Antipyril) azo]-2-naphthol (4-AAP-2-N). Iraqi National Journal of Chemistry, (43), 361-373.
[14]Affat, S. S., & Al-Shamkhawy, S. (2018). Synthesis and Characterization of a 6,6'-((1E,1'E)-(1,2- phenylenebis(azanylylidene)) bis(methanylylidene)) bis (2-methoxy-3-((6-methoxybenzo[d]thiazol-2-yl)diazenyl)phenol):as a highly sensitive reagent for determination cadmium(II) ion in the real Samples. International Journal of Pharmaceutical Research, 10(4), 480-497.

[15] Mohammed, Mohammed Qasim. "Synthesis and characterization of new Schiff bases and evaluation as Corrosion inhibitors." Journal of Basrah Researches 37.4 (2011): 116-130.

[16]Govindasamy, Rathika, and Swetha Ayappan. "Study of Corrosion inhibition properties of novel Semicarbazones on mild steel in acidic solutions." Journal of the Chilean Chemical Society 60.1 (2015): 2786-2798.

[17]Kadhim, K. J., & Munahi, M. G. (2017). Synthesis, characterization and biological evaluation of some novel Schiff's bases derived from vanillin. J. Glob. Pharma. Tech, 9(8), 383-386
[18] Köse, M., Kurtoglu, N., Gümüşsu, Ö., Tutak, M., McKee, V., Karakaş, D., & Kurtoglu, M. (2013). Synthesis, characterization and antimicrobial studies of 2-{(E)-[(2-hydroxy-5-methylphenyl) imino] methyl}-4-[(E)-phenyldiazenyl] phenol as a novel azo-azomethine dye. Journal of Molecular Structure, 1053, 89-99.
[19] Eissa, H. H. (2013). Synthesis and characterization of new azo-schiff bases and study biological activity. Journal of current research in science, 1(2), 96-103..
[20] Bambang Purwono, Chairil Anwar, and Ahmad Hanapi, synthesis of azo-imine derriveatives from vanillin as an acid base indicator. Indo. J. Chem., 2013, 13 (1), 1 – 6
[21]Jber, N. R., Abood, R. S., & Al-Dhaief, Y. A. (2011). Synthesis and spectral study of new azo-azomethine dyes and its copper (II) complexes derived from resorcinol, 4-aminobenzoylhydrazone and 4-amino antipyrine. Al-Nahrain Journal of Science, 14(4), 50-56.
[22] L.M. Vracar, D.M. Drazic, Corros. Sci. 44 (2002) 1669

[23]Loto RT Loto CA, Fedotova T (2013). Res Chem intermed 39

[24]UmorenSA,ObotIB,AkpabioLE,EtukSE(2008). Pigment and Resin Technology 37:98–105

[25]SanniO,LotoCA,PopoolaAPI(2013). Inter J Electrochem Sci 8
[26]G.Bereket, A.Yurt ,A.Balaban and B.Erk,5th **Advanced batteries and acc.umulators** –ABA-(2004).

[27]A.E.Pereira and M.F.Tavares ,**J.chromatography**, 1, 303,(2004).

[28]Jasna Halambek*, Marijana Jukić, Katarina Berković, Jasna Vorkapić-Furač, , Int. J. Electrochem. Sci., 7 (2012) 1580 - 1601.

[29] I.Ahamad, R. Prasad, M.A. Quraishi, Corros. Sci., 52 (2010) 3033 .

[30]A.Popova, Corros. Sci., 49 (2007) 2144.

[31] A.Y. El-Etre, J. Colloid Interf. Sci., 314 (2007) 578 .

[32] O.K. Abiola, A.O. James, Corros. Sci., 52 (2010) 661.

[33] L. Herrag, B. Hammouti, S. Elkadiri, A. Aounit, C. Jama, H. Vezin, F. Bentiss, Corros. Sci., 52 (2010) 3042

[34] T. Szauer and A. Brandt, ,vol.26, no.9,pp.1253–1256,1981.

[35] M. Bouklah, B. Hammouti, M. Lagren´ee, and F. Bentiss, vol.48,no.9, pp.2831–2842,2006

[36] Thabo Peme, Lukman O. Olasunkanmi, Indra Bahadur, Abolanle S. Adekunle, Mwadham M. Kabanda and Eno E. Ebenso. Molecules 2015, 20, 16004-16029

[37]J. Flis and T. Zakroczymski, Journal of the ElectrochemicalSociety ,vol.143,no.8,pp.2458–2464,1996

[38] F.Bentiss,M.Lebrini,andM.Lagrene," Corrosion Science, vol. 47, no. 12,pp.2915–2931,2005

[39]D. K. Lavanya . Frank V. Priya . D. P. Vijaya, J Fail. Anal. and Preven. (2020) 20:494–502

[40]M. Lagrenee, B.Mernari, M. Bouanis, T. Traisnel, F. Bentiss, Corros. Sci., 44 (2002) 573.

[41] E. Kraka and D. Cremer, "Computer design of anticancer drugs. A new enediyne warhead," Journal of the American Chemical Society, vol. 122, no. 34, pp. 8245–8264, 2000.

[42] I. Lukovits, E. Kalm´ an, and F. Zucchi, "Corrosion inhibitors— ´ correlation between electronic structure and efficiency," Corrosion, vol. 57, no. 1, pp. 3–8, 2001.

[43] I. Ahamad, R. Prasad, and M. A. Quraishi, "Adsorption and inhibitive properties of some new Mannich bases of Isatin derivatives on corrosion of mild steel in acidic media,"Corrosion Science, vol. 52, no. 4, pp. 1472–1481, 2010.

[44] D.K. Verma, E.E. Ebenso, M.A. Quraishi, C. Verma, Gravimetric, electrochemical surface and density functional theory study of acetohydroxamic and benzohydroxamic acids as corrosion inhibitors for copper in 1 M HCl, Results Phys. 13 (2019) 102194.

[45] O. Dagdag, A. El Harfi, O. Cherkaoui, Z. Safi, N. Wazzan, L. Guo, E.D. Akpan, C. Verma, E.E. Ebenso, R.T.T. Jalgham, Rheological, electrochemical, surface, DFT and molecular dynamics simulation studies on the anticorrosive properties of new epoxy monomer compound for steel in 1 M HCl solution, RSC Adv. 9 (2019) 4454 –4462.

[46] Li, S., Chen, S., Lei, S., Ma, H., Yu, R., Liu, D., 1999a. Corros. Sci. 41, 1273–1287. Li, S.L., Wang, Y.G., Chen, S.H., Yu, R., Lei, S.B., Ma, H.Y., Liu, D.X., 1999b. Corros. Sci. 41, 1769–1782.

[47]Li, S.L., Wang, Y.G., Chen, S.H., Yu, R., Lei, S.B., Ma, H.Y., Liu, D.X., 1999b. Corros. Sci. 41, 1769–1782.

[48] Cherry, W., Epiotis, N., Borden, W.T., 1977. Acc. Chem. Res. 10, 167– 173.

[49]Yurt, A., Bereket, G., Kıvrak, A., Balaban, A., Erk, B., 2005a. J. Appl. Electrochem. 35, 1025–1032.

[50]Yurt, A., Bereket, G., O¨g˘retir, C., 2005b. J. Mol. Struct. THEOCHEM 725, 215–221.

[51]Ali Ahmed Abdulridha a , Mahmood A. Albo Hay Allah b , Sajjad Q. Makki c , Yusuf Sertd,e , Hamida Edan Salman f and Asim A. Balakit, Journal of Molecular Liquids (2020),1-29

[52]Onuchukwu, A.I.; Njemanze, G.N. The corrosion susceptibility of dyes and dye-bath auxiliaries on galvanized steel pipes. J. Chem. Soc. Niger. 1997, 22, 1500–1504.

[53]Ebenso, E.E. Inhibition of corrosion of mild steel hydrochloric acid by some azo dyes. Niger. J. Chem. Res. 2001, 6, 8–12.

[54]Oguzie, E.E.; Unaegbu, C.; Ogukwe, C.E.; Okolue, B.N.; Onuchukwu, A.I. Inhibition of mild steel corrosion in sulphuric acid using indigo dye and synergistic halide additives. Mater. Chem. Phys. 2004, 84, 363–368.

[55] Ebenso, E.E.; Okafor, P.C.; Ibok, U.J.; Ekpe, U.J.; Onuchukwu, A.I. The joint effects of halide ions and methylene blue on the corrosion inhibition of aluminium and mild steel in acid corrodent. J. Chem. Soc. Niger. 2004, 29, 15–25.

[56] L. Herrag, B. Hammouti, S. Elkadiri, A. Aouniti, C. Jama, H. Vezin and F. Bentiss, Adsorption properties and inhibition of mild steel corrosion in hydrochloric solution by some newly synthesized diamine derivatives: experimental and theoretical investigations, Corros. Sci., 2010, 52, 3042–3051.

[57] L.C.laa, J.kryzsen, Anna stochmal ,W.oleszek ,M. Waksmun - dzka -Hajnosa, Journal of Pharmaceutica and Biomedical Analysis, 70, 126 135, 2012.

[58] Qasim, Maytham T., and Hussein Khudair Al-Mayali. "Investigate the relation between Baicalin effect and Gene expression of LH, FSH, Testosterone in male rats treated with Gemcitabine drug." *Research Journal of Pharmacy and Technology* 12.9 (2019): 4135-4141.

[59] Qasim, Maytham T., and Hussein Khudair Al-Mayali. "The immunological and protective role of Baicalin in male rats treated with chemotherapy (Gemcitabine)." *Journal of Physics: Conference Series*. Vol. 1234. No. 1. IOP Publishing, 2019.

[60] Tahmasebi S, Qasim MT, Krivenkova MV, et al. The effects of Oxygen-Ozone therapy on regulatory T-cell responses in multiple sclerosis patients [published online ahead of print, 2021 Mar 16]. *Cell Biol Int*. 2021;10.1002/cbin.11589. doi:10.1002/cbin.11589.